

A search for binarity using *FUSE* observations of DAO white dwarfs

S.A. Good^{1*}, M.A. Barstow¹, M.R. Burleigh¹, P.D. Dobbie¹ and J.B. Holberg²

¹*Department of Physics and Astronomy, University of Leicester, University Road, Leicester LE1 7RH*

²*Lunar and Planetary Laboratory, University of Arizona, Tucson, AZ 85721, USA*

Released 2002 Xxxxx XX

ABSTRACT

We report on a search for evidence of binarity in *Far-Ultraviolet Spectroscopic Explorer* (*FUSE*) observations of DAO white dwarfs. Spectra recorded by *FUSE* are built up from a number of separate exposures. Observation of changes in the position of photospheric heavy element absorption lines between exposures, with respect to the stationary interstellar medium lines, would reveal radial velocity changes - evidence of the presence of a binary system. This technique is successful in picking out all the white dwarfs already known to be binaries, which comprise 5 out of the sample of 16, but significant radial velocity shifts were found for only one additional star, Ton 320. This object is also known to have an infrared excess (Holberg & Magargle 2005). DAOs can be separated broadly into low or normal mass objects. Low mass white dwarfs can be formed as a result of binary evolution, but it has been suggested that the lower mass DAOs evolve as single stars from the extended horizontal branch (Bergeron et al. 1994), and we find no evidence of binarity for 8 out of the 12 white dwarfs with relatively low mass. The existence of higher mass DAOs can also be explained if they are within binary systems, but of the four higher mass stars in the sample studied, PG 1210+533 and LB 2 do not exhibit significant radial velocity shifts, although there were only two exposures for the former object and the latter has an infrared excess (Holberg & Magargle 2005).

Key words: stars: atmospheres - white dwarfs - ultraviolet: stars.

1 INTRODUCTION

DAO white dwarfs, the prototype of which is HZ 34 (Koester, Weidemann, & Schulz 1979; Wesemael et al. 1993), are a group of white dwarfs that are observed to have both hydrogen and helium lines in their optical spectra, in contrast to the more common DAs, which exhibit only hydrogen absorption. Hence, the presence of detectable He must arise from the existence of a thin overlying H envelope or there must be a mixing process, dredging up He from the deeper layers of the stellar photosphere. Radiative forces appear to be too low to support sufficient quantities of helium to be able to produce the observed lines (Vennes et al. 1988). A thin H envelope might arise through float up of residual H in a He-rich DO atmosphere as objects transfer between the helium and hydrogen cooling channels (Fontaine & Wesemael 1987). However, the discovery by Napiwotzki & Schöberner (1993) that the He II line in the optical spectra of one DAO was better reproduced by a homogeneous rather than a layered atmospheric model was contrary to this view. Bergeron et al. (1994) performed a similar comparison on a sample of 14 DAOs, but found only one object for which a stratified model was preferred. Of the remaining objects, most were found to be comparatively hot and low gravity, implying they have low mass. Therefore, the progenitors of some of these DAOs are unlikely to have had sufficient mass to ascend

the asymptotic giant branch (AGB), and instead they may have evolved from extended horizontal branch stars. It was suggested that, in these stars, weak mass loss may be occurring, a process that might be able to support the observed quantities of helium in the line forming regions of the DAOs (Unglaub & Bues 1998, 2000). Three objects (RE 1016-053, PG 1413+015 and RE 2013+400) were in close binary systems and have M dwarf (dM) companions. These have ‘normal’ temperatures and gravities, yet still have detectable helium lines in their optical spectra. This may be because mass is lost as the progenitor star passes through the common envelope phase, leading to the star being hydrogen poor, and allowing a weak process, such as mass loss, to mix helium into the line forming region of the white dwarf. Alternatively, these DAOs might be accreting from the wind of their companions - RE 0720-318, another DAO with a dM companion, has been shown to have changing helium abundance over time, which might be due to episodic accretion (Finley, Koester, & Basri 1997; Vennes, Thorstensen, & Polomski 1999). In addition, Dobbie et al. (1999) identified likely spatial non-uniformities in the surface abundance of helium, which are consistent with models of accretion. Finally, for one star in the Bergeron et al. (1994) sample (PG 1210+533), the He II line profile was not reproduced satisfactorily by either chemically homogeneous or stratified models. In addition, its helium line strengths have been observed to change over a time period of ~ 15 years (Bergeron et al. 1994). This is not a high temperature, low gravity object (Bergeron et al. 1994;

* Email: sag15@le.ac.uk

Good et al. 2004), and has no infrared excess that might indicate a companion star, so it does not appear to fit in with any of the other DAOs.

Therefore, DAO white dwarfs form a relatively heterogeneous group. For some, the existence of cool, non-degenerate companions may play a significant role in the presence of photospheric He, either from prior common envelope evolution or from ongoing mass transfer. We investigate a sample of 16 DAO white dwarfs to determine how many exhibit evidence of short term radial velocity variations and thus may be members of close binary systems, using *Far-Ultraviolet Spectroscopic Explorer (FUSE)* data. *FUSE* spectra are built up from a number of exposures that last up to 90 minutes, which need to be combined to achieve the desired signal-to-noise of the proposer. Although the signal-to-noise of these exposures is far worse than in the final combined spectrum, strong interstellar and photospheric absorption features can still be identified. This investigation exploits this fact to search for radial velocity shifts in photospheric lines relative to the stationary interstellar medium lines, which might indicate the presence of short period binary systems.

2 OBSERVATIONS

Far-ultraviolet (far-UV) data for all the objects were recorded by the *FUSE* spectrographs. Table 1 lists the observations that were used, which were downloaded by us from the Multimission Archive (<http://archive.stsci.edu/mast.html>), hosted by the Space Telescope Science Institute. Overviews of the mission and in-orbit performance have been published by Moos et al. (2000) and Sahnou et al. (2000) respectively; below is a brief description of the instrument.

The *FUSE* instrument contains four separate co-aligned optical paths (channels), each having a mirror, a focal plane assembly and a diffraction grating, whose dispersed images share a portion of a detector. Light from the target enters into the apertures of all the channels simultaneously. To obtain optimal coverage over the full hydrogen Lyman series (apart from α), two of the mirrors and two of the gratings are coated with LiF over a layer of aluminium, while the others are coated with SiC since the reflectivity of the Al+LiF is low below $\sim 1020 \text{ \AA}$. Two microchannel plate detectors (1 and 2) are used, with each subdivided into two segments (A and B), which are separated by a small gap. Light from a SiC and a LiF channel falls onto each detector, resulting in 8 individual spectra. Thermal changes can result in rotations of the mirrors, hence most observations are carried out with the largest available aperture (LWRS, 30×30 arcsec) to prevent the target drifting outside the aperture. In this aperture the point source resolution has been found to be 20 000 for the LiF 1 channel (*The FUSE observers guide* – see <http://fuse.pha.jhu.edu/>). There are two modes for recording data – time-tagged event lists (TTAG data) or as spectral image histograms (HIST data), which are used where the source is bright. As *FUSE* is in a low-Earth orbit emission lines from the Earth’s atmosphere are sometimes seen, which must be dealt with during the data analysis. A particular problem with *FUSE* spectra is the presence of the ‘worm’, which is a shadow cast by the electron repeller grid located above the detector surface, and manifests itself by a decrease in flux by up to 50 per cent, particularly in the LiF 1B segment. The amount of flux loss varies according to how closely the position of the grid wires coincides with the image, and is also affected by the position of the target in the aperture and so cannot easily be removed by the calibration software.

Table 2. ISM lines used to correct for wavelength calibration shifts between *FUSE* exposures, with rest frame wavelengths as listed by Morton (1991).

Species	Lab. wavelength / \AA
O I	988.6549
Si II	989.8731
Si II	1020.6989
C II	1036.3367
C II	1037.0182
O I	1039.2304
Ar I	1048.2199
Fe II	1063.1764
Ar I	1066.6599

As a number of improvements have been made to the calibration pipeline since the data were originally processed and archived, after they were downloaded the data were reprocessed using a locally installed version of the CALFUSE pipeline (version 2.0.5 or later). It was found that the wavelength calibration of each segment did not perfectly match with the others, so only data from the LiF 1A combination of mirrors and detectors were used. This should have the best calibration since it is used in the pointing of the telescope.

The sample consists of 16 DAO white dwarfs. Temperatures and gravities for these stars have previously been published by Good et al. (2004). In the sample, 5 are known binaries: RE 0720-318 (Vennes & Thorstensen 1994; Barstow et al. 1995), PG 0834+500 (Saffer, Livio, & Yungelson 1998), HS 1136+6646 (Heber, Dreizler, & Hagen 1996), RE 2013+400 (Pounds et al. 1993; Barstow et al. 1995), and the double-degenerate Feige 55 (Holberg et al. 1995). These stars are included in this analysis to assess the ability of the technique to detect white dwarfs in binary systems. In addition, Ton 320 and LB 2 have known infrared excesses that might indicate a companion (Holberg & Magargle 2005).

3 METHODOLOGY

Only the LiF 1A segment is used in this experiment as it is the best calibrated. Even so, the wavelength scale can drift between exposures; this can be corrected for by reference to interstellar medium (ISM) lines, the radial velocity of which should be constant. The lines used are listed in Table 2, with their rest frame wavelengths from Morton (1991). Several of the lines were detectable in the spectra of every object. A Gaussian and a second order polynomial were used to model the line profile and continuum level respectively. The set of parameters that best reproduce the data were determined by a least-squares fitting routine that is part of the IDL language (CURVEFIT). In addition, a 1σ error on the central wavelength was returned by the fitting function. As the true redshift of the ISM lines is not known, and the *FUSE* wavelength calibration is insufficiently accurate, the mean position of the interstellar lines was taken to be the correct absolute calibration. The central wavelengths of photospheric lines were then measured in a similar way. Table 3 lists the lines used, although again not all were present in all the objects, or were difficult to identify in the low signal-to-noise exposures. In addition, in lines of sight where the Ar I ISM line at 1066.6599 \AA was observed, the Si IV was indiscernible due to line blending. Wavelength corrections, calculated from the positions of the ISM lines in each exposure, were applied to each measured central wavelength, the velocity of the lines were calculated, and finally the mean radial velocity for each exposure was calculated.

Table 1. List of *FUSE* observations for the stars in the sample.

Object	WD number	Obs. ID	Date	Length / s	Aperture	TTAG/HIST
A 7	WD0500-156	B0520901000	2001/10/05	11525	LWRS	TTAG
HS 0505+0112	WD0505+012	B0530301000	2001/01/02	7303	LWRS	TTAG
PuWe 1	WD0615+556	B0520701000	2001/01/11	6479	LWRS	TTAG
		S6012201000	2002/02/15	8194	LWRS	TTAG
RE 0720-318	WD0718-316	B0510101000	2001/11/13	17723	LWRS	TTAG
TON 320	WD0823+317	B0530201000	2001/02/21	9378	LWRS	TTAG
PG 0834+500	WD0834+501	B0530401000	2001/11/04	8434	LWRS	TTAG
A 31		B0521001000	2001/04/25	8434	LWRS	TTAG
HS 1136+6646	WD1136+667	B0530801000	2001/01/12	6217	LWRS	TTAG
		S6010601000	2001/01/29	7879	LWRS	TTAG
Feige 55	WD1202+608	P1042105000	1999/12/29	19638	MDRS	TTAG
		P1042101000	2000/02/26	13763	MDRS	TTAG
		S6010101000	2002/01/28	10486	LWRS	TTAG
		S6010102000	2002/03/31	11907	LWRS	TTAG
		S6010103000	2002/04/01	11957	LWRS	TTAG
		S6010104000	2002/04/01	12019	LWRS	TTAG
PG 1210+533	WD1210+533	B0530601000	2001/01/13	4731	LWRS	TTAG
LB 2	WD1214+267	B0530501000	2002/02/14	9197	LWRS	TTAG
HZ 34	WD1253+378	B0530101000	2003/01/16	7593	LWRS	TTAG
A 39		B0520301000	2001/07/26	6879	LWRS	TTAG
RE 2013+400	WD2013+400	P2040401000	2000/11/10	11483	LWRS	TTAG
DeHt 5	WD2218+706	A0341601000	2000/08/15	6055	LWRS	TTAG
GD 561	WD2342+806	B0520401000	2001/09/08	5365	LWRS	TTAG

Table 3. Photospheric lines used to measure radial velocities.

Species	Lab. wavelength / Å
P v	997.5240
O vI	1031.9310
O vI	1037.6130
Si IV	1066.6140
O IV	1067.7680
Fe VII	1073.9480

Once the radial velocities had been measured, a test was performed to measure the significance of any differences found. To do this, a constant velocity line was fitted to the radial velocity measurements and the value of the χ^2 statistic recorded. Then, this was compared to a simulation of how the data would look if the radial velocity of the object were constant, but with the measurements perturbed by random errors. To do this, randomly generated Gaussian distributed errors were calculated, the standard deviation of which was set equal to the error in each of the real radial velocity measurements, since the accuracy of the measurements depend on the length of exposure and number of lines used, and varied between measurements. A constant velocity line was then fit to the simulated measurements and the χ^2 measured, and this was then compared to the χ^2 of the fit to the real measurements to see if the observations could be explained by measurement error alone, without having to invoke motion in a binary. This was done 10^6 times and the number of times that the simulated χ^2 exceeded that of the real χ^2 was measured. If this occurred in less than 99.7% of times, the radial velocity differences were taken to be significant at the 3σ level.

4 RESULTS

Table 4 lists the results of the radial velocity measurements and significance tests, and indicates whether or not the objects were

already known to be in binary systems. The technique has successfully picked out all of the known binaries, and Figure 1 shows the radial velocity measurements for each of these stars. The radial velocity changes are clearly evident in each, although, of these, only Feige 55 has greater than 10 measurements, and has a complete orbit of radial velocity measurements, allowing the period and amplitude of the variations to be measured. The best fitting sine curve to the data was determined using the IDL CURVEFIT function, which uses a χ^2 minimisation technique to determine the best fit model parameters to a function. The radial velocity of the white dwarf can be expressed in the following way:

$$v(t) = v_0 + v_{max} \sin \left[\frac{2\pi(t - t_0)}{P} \right]$$

where the radial velocity v at time t is dependent on the system velocity v_0 , the velocity semi-amplitude v_{max} , the system period P , and the epoch t_0 . Since the *FUSE* observations were widely spaced in time relative to the period, the best fitting parameters, in particular the epoch, are very sensitive to the period and simultaneously fitting the period, epoch, velocity semi-amplitude and system velocity leads to unpredictable results. Instead, the system velocity and velocity semi-amplitude were fit to the data for a range of periods and epochs, and the parameters that provided the least reduced χ^2 of all the fits were recorded. The results are shown in Figure 2; the best fitting period, velocity semi-amplitude and system velocity are 1.493 days, 74.99 km s⁻¹ and -0.685 km s⁻¹ respectively. This compares with 1.493 days, 77.4 km s⁻¹ and 0.1 km s⁻¹ measured by Holberg et al. (1995) from optical and *International Ultraviolet Explorer (IUE)* data, and a period of 1.489 days, velocity semi-amplitude of 80.377 km s⁻¹ and system velocity of -1.19 km s⁻¹ found by Kruk, Chayer, & Dupuis (2003), using *FUSE* data. In our calculation, t_0 , which is the reference epoch when the radial velocity equalled the system velocity and when the radial velocity is increasing, was at 2451601.762 (heliocentric Julian date). Although the figure shows that visually the sine curve provides a good match

Table 4. Results of the Monte Carlo analysis. Those objects that the calculations suggest have real radial velocity shifts at the 3σ level are underlined. The stars in bold are already known to have companions.

Object	Number of exposures	Best fitting vel / km s ⁻¹	Chance of variations occurring randomly
A 7	5	38.8	0.01540
HS 0505+0112	3	50.4	0.02695
PuWe 1	6	17.5	0.07894
<u>RE 0720-318</u>	5	-194.4	0.00000*
<u>TON 320</u>	9	33.8	0.00000*
<u>PG 0834+500</u>	3	-46.6	0.00001
A 31	4	80.8	0.01788
<u>HS 1136+6646</u>	4	53.2	0.00000*
<u>Feige 55</u>	41	4.2	0.00000*
PG 1210+533	2	-3.3	0.93316
LB 2	5	15.1	0.00882
HZ 34	4	6.7	0.56639
A 39**	3	2.2	0.36889
<u>RE 2013+400</u>	9	-15.2	0.00000*
DeHt 5**	2	-40.9	0.65238
GD 561	2	-12.5	0.61473

* In none of the Monte Carlo trials was the minimum χ^2 achieved by fitting a constant velocity line to the real data less than the χ^2 from fitting a constant velocity line to the simulated data.

** Velocity measurements made difficult by H₂ absorption.

to the data, the reduced χ^2 statistic comparing the sine curve to the data is 23, indicating that the formal errors returned by the fitting function underestimated the true errors inherent in the technique; in addition, the fact that the fit statistic does not take into account that each exposure lasts ~ 90 minutes, rather than being discrete measurements, may be contributing to the high value.

Orbital parameters for RE 0720-318 and RE 2013+400 have been published by Vennes, Thorstensen, & Polomski (1999). These parameters can be used to predict the radial velocity of the white dwarfs at the time of the *FUSE* observations in order to check for consistency with our radial velocity measurements. For RE 0720-318, it was noted that the predicted radial velocities were out of phase with the measurements by a small amount, and that the magnitudes of the velocities were also slightly different. To quantify these differences the set of parameters that best matched the measured quantities were found by searching around the values given by Vennes, Thorstensen, & Polomski (1999). Predicted radial velocities were calculated for values between $\pm 3\sigma$ of the Vennes, Thorstensen, & Polomski (1999) quantities for the time when the velocities increase through their mean value and the velocity semi-amplitude of the orbit. The value of the orbital period was not varied since Vennes, Thorstensen, & Polomski (1999) quote this number to high precision, and a change of 1σ in the period resulted in a change in χ^2 of only < 0.001 . Since the *FUSE* observations sample only a limited part of the white dwarf orbit, there is insufficient information to find both the mean radial velocity and velocity semi-amplitude. Therefore, we also did not attempt to vary the mean radial velocity from the value given by Vennes, Thorstensen, & Polomski (1999). For each combination of parameters, χ^2 was calculated, and the set of parameters that gave the lowest χ^2 recorded. This resulted in the following set of parameters for the orbit of RE 0720-318: reference Julian date when the radial velocities increase through the mean, 2452226.649 (a decrease compared to the Vennes, Thorstensen, & Polomski (1999) ephemeris of 1.38 of their sigmas), mean white dwarf radial velocity, 51.7 km s⁻¹, velocity semi-amplitude, 81.8 km s⁻¹

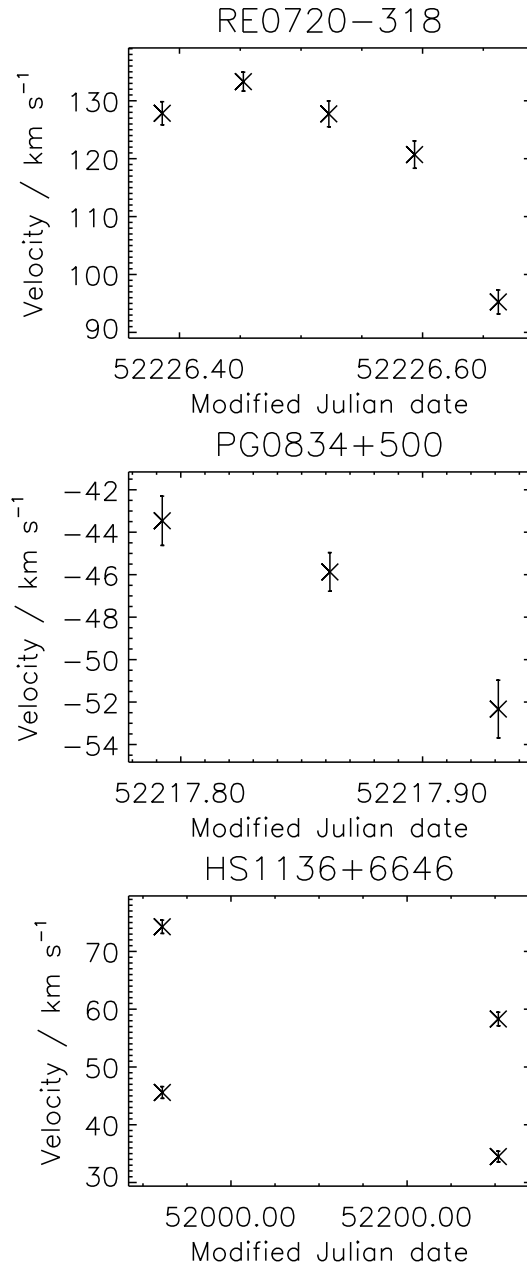


Figure 1. Plots of the radial velocity measurements made for the white dwarfs that are known to be in binary systems.

(1.62σ higher than the Vennes, Thorstensen, & Polomski (1999) value, although this will also incorporate any error in the mean velocity), and period, 1.26243 days. The χ^2 for these parameters is 3.95, compared to 140.97 for the values given by Vennes, Thorstensen, & Polomski (1999). Figure 3 shows the measured radial velocities for RE 0720-318 and the velocities that were predicted using these parameters.

The procedure described above was also followed for RE 2013+400. However, for this object the *FUSE* observations cover a greater proportion of the orbit than for RE 0720-318. It was therefore possible to vary the period and mean radial velocity from the numbers given by Vennes, Thorstensen, & Polomski (1999) to obtain values for these parameters also. The set of orbital parameters found for RE 2013+400 were: reference Julian date when ve-

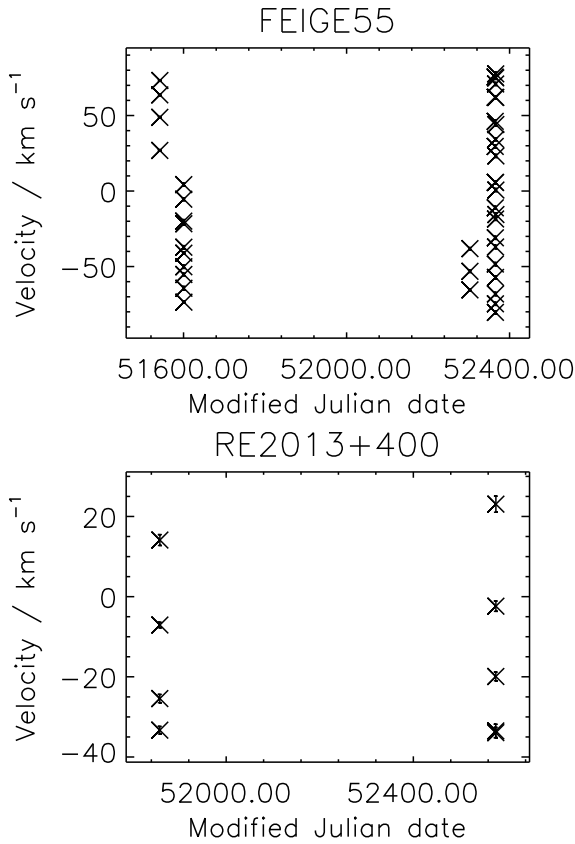


Figure 1 – continued

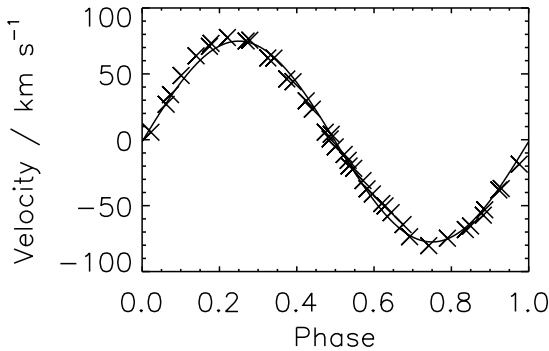


Figure 2. Feige 55 radial velocities folded onto the best fitting period, with a sine curve overplotted.

locities increase through the mean, 2451858.081 (0.35σ greater than the Vennes, Thorstensen, & Polomski (1999) value), mean radial velocity, 1.1 km s^{-1} ($+1.26\sigma$), velocity semi-amplitude, 35.2 km s^{-1} ($+2.13\sigma$), and period, 0.705521 days ($+0.29\sigma$, although this change improved χ^2 by only 0.44). χ^2 for this set of parameters is 6.11, compared to 35.47 for the Vennes, Thorstensen, & Polomski (1999) values. Figure 4 shows the measured and predicted velocities for this object. These results suggest that the radial velocities measured from *FUSE* data are reliable and are consistent with the published orbital parameters. Even with the limited number of radial velocity measurements available it was possible to refine the

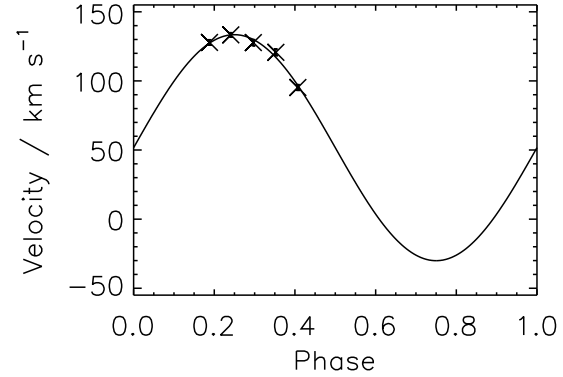


Figure 3. RE0720-318 radial velocities folded onto the period, with the predicted radial velocities overplotted.

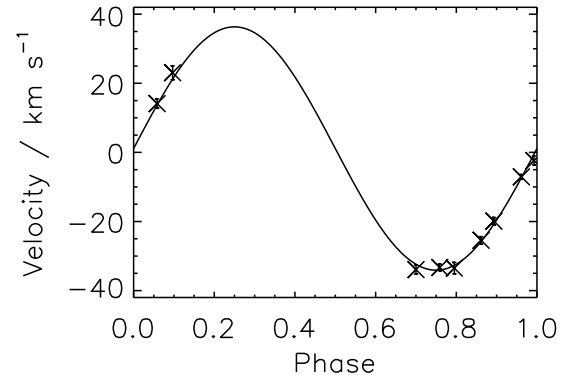


Figure 4. RE2013+400 radial velocities folded onto the period, with the predicted radial velocities overplotted.

orbital parameters, suggesting that *FUSE* data could potentially be used in the future to improve the ephemerides for stars.

The sixth object for which significant radial velocity changes were found was Ton 320, which has an infrared excess and thus is suspected to be within a binary system (Holberg & Magargle 2005). The radial velocity measurements for this object are shown in Figure 5. In contrast to the radial velocity measurements for the known binaries, shown in Figure 1, the radial velocities seen for Ton 320 appear relatively constant, apart from the second, sixth and seventh measurements out of the total of nine, and no sinusoidal nature to the velocity shifts is obvious. Therefore, it is possible that this is a spurious detection of radial velocity changes, due to an underestimation of the errors in the radial velocity measurements. Alternatively, this object may be within a binary system, with the sinusoidal nature of the radial velocity variations hidden within the errors, or by the separation of the exposures. To investigate this possibility, the range of periods to which the radial velocity measurement technique is sensitive for this object was first found. To determine this, the radial velocity changes that would occur between the observations made by *FUSE* were calculated for situations where the object was assumed to be in a binary system with a number of different inclinations and at a number of different phases at the time of first observation. The white dwarf was assumed to have a mass of $0.5 M_{\odot}$, while a conservative value of $0.1 M_{\odot}$ was assumed for the companion; a more massive companion will result in larger ra-

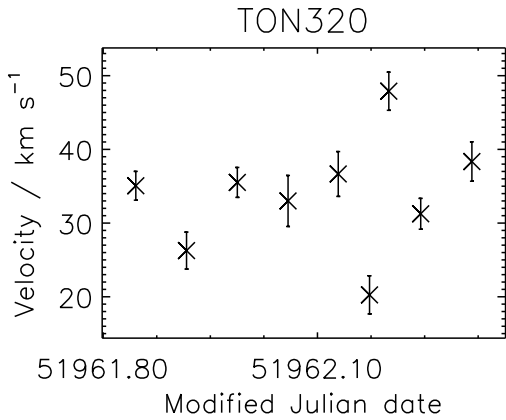


Figure 5. Plots of the radial velocity measurements made for Ton 320, which is a suspected binary, and for which significant radial velocity changes were detected.

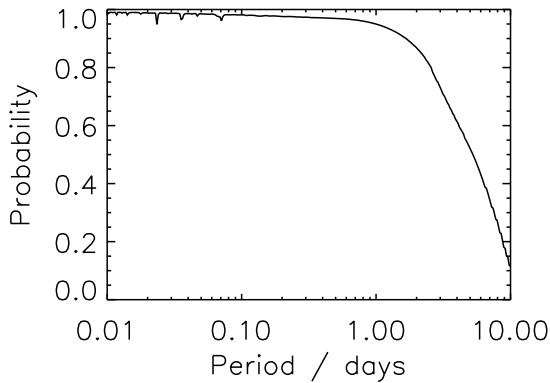


Figure 6. The probability that radial velocity measurements would be detected from the data for Ton 320.

dial velocity shifts. The radial velocity shift that was assumed to be detectable was set to the maximum error in the velocity measurements for the object (3.46 km s^{-1} for Ton 320). For each period, the number of times where radial velocity changes would be detectable was counted and normalised relative to the total number of trials, with the results plotted in Figure 6. The plot demonstrates that there is a greater than 90% probability that if Ton 320 is within a binary system with period less than one day, radial velocity variations would be observed within the measurements. However, this does not preclude the possibility that Ton 320 may be in such a binary system but with weak radial velocity variations because, for example, it is at an unfavourable inclination, making them difficult to detect.

To determine if it is possible that the radial velocity measurements do follow a sinusoidal pattern, a procedure identical to that used to determine the best fitting sine curve to the Feige 55 velocities was used. The best fitting curve had the following parameters: period, 0.037 days, epoch when radial velocities increase through the mean value, 2451961.535, velocity semi-amplitude, 15.95 km s^{-1} , and system velocity, 44.99 km s^{-1} . The reduced χ^2 of the fit is <4 , much less than that obtained for Feige 55, which, if the errors on the radial velocity measurements are underestimated, suggests that noise is being fitted. In addition, this period is very short compared to, for example, the systems listed

by Hillwig, Honeycutt, & Robertson (2000). However, other solutions that provide higher values of χ^2 are possible, but more closely spaced measurements are required to constrain the fit and to determine with certainty if Ton 320 lies within a close binary system.

The remaining objects are those for which no significant radial velocity changes were found. However, the significance test for radial velocity changes was only narrowly failed by a number of these: A 7, HS 0505+0112, PuWe 1, A 31 and LB 2 (which Holberg & Magargle (2005) identified as having an infrared excess), for which the result of the significance test was <0.1 . The radial velocity measurements for these objects are shown in Figure 7. Finally, radial velocity plots for PG 1210+533, HZ 34, A 39, DeHt 5 and GD 561, for which the results of the significance tests were >0.1 , are shown in Figure 8. However, none of these objects have more than 6 exposures, which limits the sensitivity of the method; Figure 9 demonstrates the probability of detecting radial velocity shifts for periods between 0.1 and 10 days, for PuWe 1, PG 1210+533 and LB 2. PG 1210+533 has only two exposures from a single *FUSE* observation, and therefore our method for detecting binarity is least sensitive for this object, with the sensitivity beginning to decline above 0.1 days and strongly decreasing where the period is a multiple of the separation in time of the exposures. For LB 2, with five exposures, a better than 90% chance of detecting radial velocity changes if it were within a binary system for period up to 1 day, and with the additional exposures, the separation in time of the measurements is less significant. PuWe 1 has six exposures, but these were recorded in two observations, separated in time by over a year. The probability of detecting radial velocity changes is limited by this separation in time and, although better than for PG 1210+533, the five continuous measurements for LB 2 provides the best chance of detecting radial velocity shifts less than a day. Therefore, to improve the significance of these non-detections of radial velocity shifts, longer observations are required.

5 DISCUSSION

Evidence for binarity has been found for only 6 DAOs. These 6 are all known, or suspected to be in binary systems from other observations. This suggests that the technique we have adopted is a valid way of searching for binarity in the remainder of the sample. DAO white dwarfs can broadly be separated into two categories: ‘normal’ mass white dwarfs, generally in binary systems, or low mass stars with possible winds. To investigate what category each DAO falls into, we calculate the mass of each white dwarf by combining the temperatures and gravities measured by Good et al. (2004) with the evolutionary models of Bloeker (1995) and Driebe et al. (1998); these are listed in Table 5. Since Good et al. (2004) found differences between the best fitting model to their optical and far-UV data, we list mass estimates from both. This introduces a large uncertainty in the mass measurements, with the *FUSE* estimates generally higher, and in some cases up to $0.2 M_{\odot}$ different to the optical measure. To simplify the discussion, we use the optical mass here, since the mass could not be calculated for three objects (PG 0834+500, HS 1136+6646 (see also Sing et al. 2004) and HS 0505+0112) from *FUSE* data as their temperatures were so extreme. It should be noted that if the *FUSE* masses are correct, most of the DAOs would have a relatively ‘normal’ mass for a white dwarf, although they are hotter than a typical DA, and so would be post-AGB stars, rather than having to have evolved from the extended horizontal branch or in a binary system. We divide the

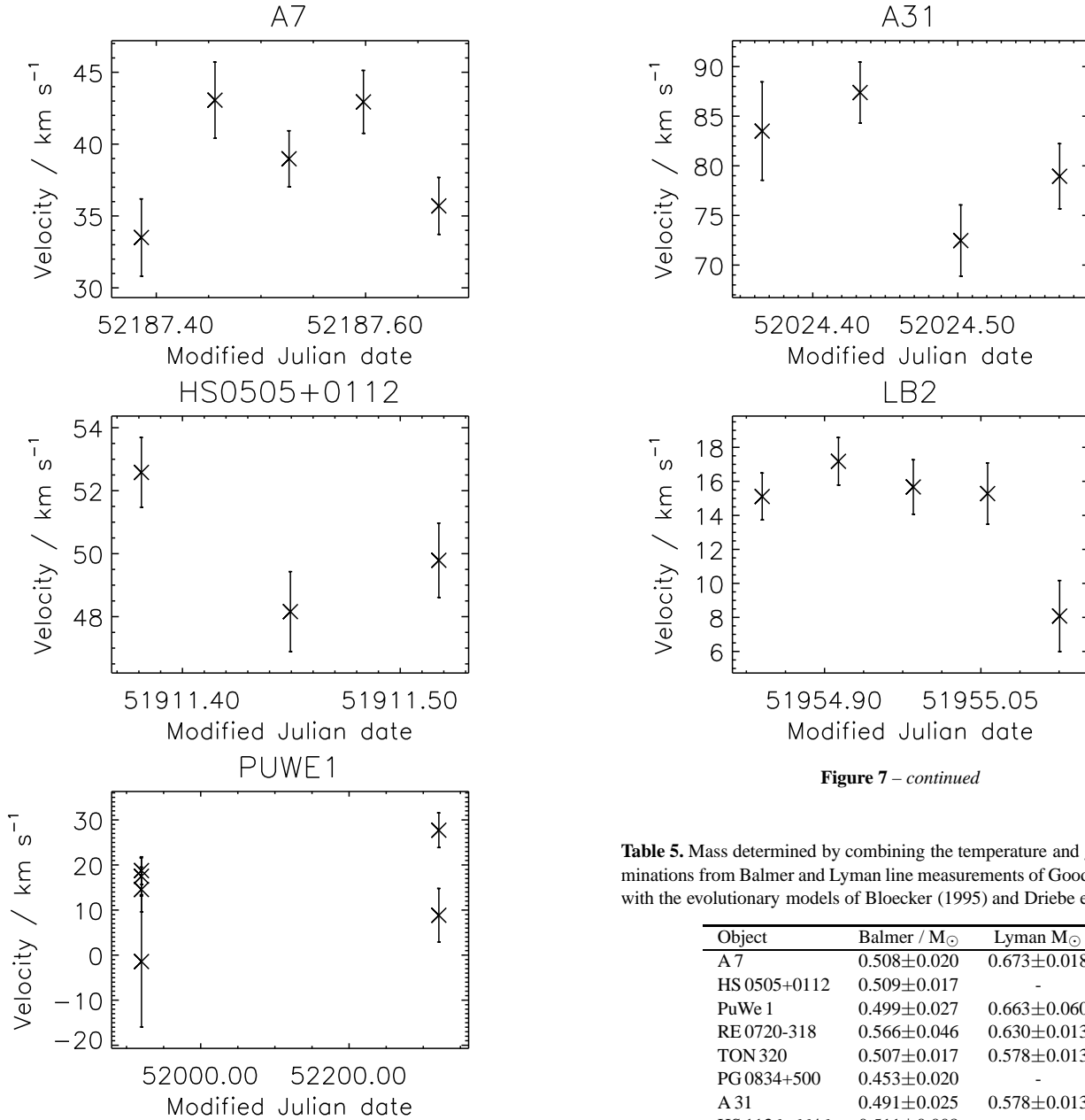


Figure 7 – continued

Figure 7. Plots of the radial velocity measurements made for objects where the chances of the radial velocity variations occurring randomly were less than 0.1.

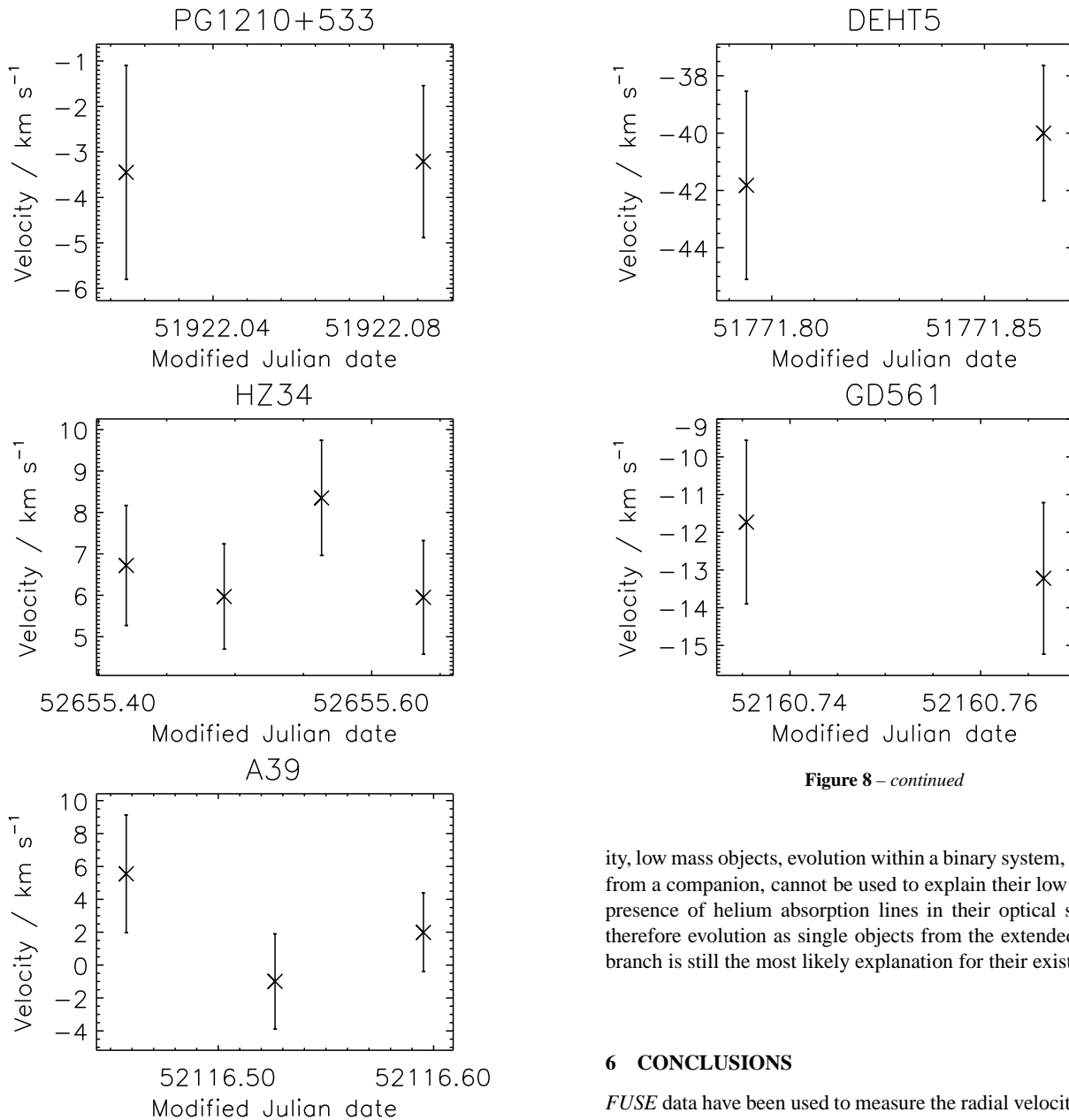
objects into groups; the higher mass stars all have $> 0.55 M_{\odot}$ from the optical measurements, while the remainder are put into a lower mass group.

Of the DAOs with comparatively high mass, evidence for binarity was found for RE 0720-318 and RE 2013+400 (both of which are DAO+dM binaries), but not for PG 1210+533 and LB 2. Only two exposures were obtained for PG 1210+533, while LB 2 has 5, and it might be possible that radial velocity shifts were missed because the separation in time of exposures was insufficient, because the system was viewed at an unfavourable phase, or if the radial velocity measurement technique were insufficiently sensitive. In addition, if a system is at high inclination, no radial velocity variations would be detectable. This may indeed be the case for LB 2,

Table 5. Mass determined by combining the temperature and gravity determinations from Balmer and Lyman line measurements of Good et al. (2004) with the evolutionary models of Bloeker (1995) and Driebe et al. (1998).

Object	Balmer / M_{\odot}	Lyman M_{\odot}
A 7	0.508 ± 0.020	0.673 ± 0.018
HS 0505+0112	0.509 ± 0.017	-
PuWe 1	0.499 ± 0.027	0.663 ± 0.060
RE 0720-318	0.566 ± 0.046	0.630 ± 0.013
TON 320	0.507 ± 0.017	0.578 ± 0.013
PG 0834+500	0.453 ± 0.020	-
A 31	0.491 ± 0.025	0.578 ± 0.013
HS 1136+6646	0.511 ± 0.008	-
Feige 55	0.439 ± 0.017	0.518 ± 0.002
PG 1210+533	0.595 ± 0.031	0.590 ± 0.022
LB 2	0.557 ± 0.049	0.521 ± 0.009
HZ 34	0.417 ± 0.019	0.477 ± 0.032
A 39	0.455 ± 0.036	0.531 ± 0.018
RE 2013+400	0.642 ± 0.046	0.661 ± 0.009
DeHt 5	0.470 ± 0.024	0.412 ± 0.018
GD 561	0.464 ± 0.029	0.442 ± 0.023

which was identified by Holberg & Magargle (2005) as having an infrared excess. It should also be noted that for this object the mass determined from the Lyman line results is lower than that obtained from the Balmer line results and using the lower mass would place LB 2 in the lower mass group. As shown in Figure 9, since there are fewer exposures for PG 1210+533, the method is less sensitive than for LB 2. However, it is still 80% likely that radial velocity shifts would be detected by this experiment if it were in a binary system with period less than almost a day, unless its period hap-

**Figure 8** – *continued***Figure 8.** Plots of the radial velocity measurements for stars where the chances of the observed changes in radial velocity occurring randomly were greater than 0.1.

pened to match the separation of exposures in time, or a multiple of that separation. This indicates that this method is quite a sensitive way of searching for white dwarfs in binary systems, particularly if a number of exposures have been made, and hence it is unlikely, although not impossible, that PG 1210+533 is in a short period binary system, hence the explanation for helium in the spectrum of PG 1210+533 is still elusive.

In the observations of the remaining 12 white dwarfs, evidence of binarity was found for only Ton 320, PG 0834+500, HS 1136+6646 and Feige 55, which are all known or suspected binary stars. Although low mass white dwarfs can be formed within in binary systems, these results suggest that not all of these have companions. Therefore, for most of the high temperature, low grav-

ity, low mass objects, evolution within a binary system, or accretion from a companion, cannot be used to explain their low mass or the presence of helium absorption lines in their optical spectra, and therefore evolution as single objects from the extended horizontal branch is still the most likely explanation for their existence.

6 CONCLUSIONS

FUSE data have been used to measure the radial velocity variations in 16 DAO white dwarfs, from the position of the photospheric heavy element absorption lines in their spectra. The technique was found to be successful in detecting radial velocity variability in all the known binaries, and even with only 2 exposures there is better than a 80% chance of observing velocity changes if the period of the system is less than a day, apart from where the period is a multiple of the temporal separation of exposures.

Radial velocity variations were only detected for those objects already known or suspected to be binaries, although it is possible that some of the others possess binary companions that are too highly inclined, or which were observed at unfavourable phases or have orbital periods too long with respect to the time span covered by our observations to be detected. Of the low mass DAOs, significant changes in radial velocity were observed for only four of the twelve objects, suggesting that the majority of this type of DAO do not exist in binary systems and may therefore have evolved as single stars from the extended horizontal branch. No evidence of binarity was found for two of the four higher mass white dwarfs in the sample. One of these objects, LB 2, has an infrared excess and

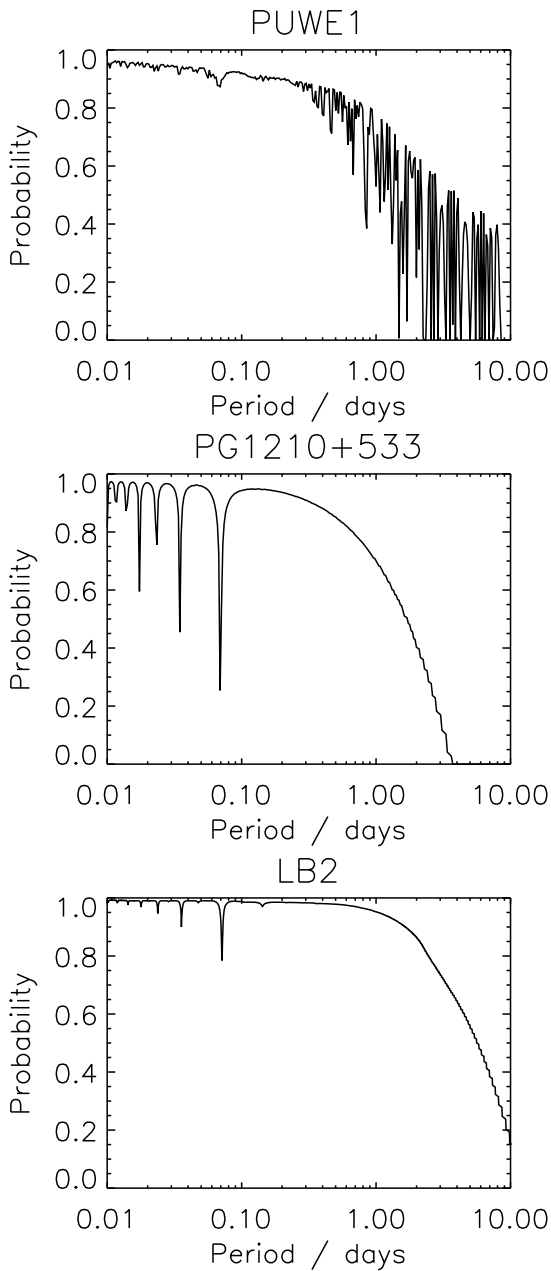


Figure 9. The probability of detecting radial velocity variations for PuWe 1, PG 1210+533 and LB 2.

hence may in fact have a companion. The presence of helium in the spectrum of the other, PG 1210+533, is still unexplained.

ACKNOWLEDGMENTS

Based on observations made with the NASA-CNES-CSA Far Ultraviolet Spectroscopic Explorer. *FUSE* is operated for NASA by the Johns Hopkins University under NASA contract NAS5-32985. SAG, MAB, MRB and PDD were supported by PPARC, UK; MRB acknowledges the support of a PPARC Advanced Fellowship. JBH wishes to acknowledge support from NASA grants NAG5-10700 and NAG5-13213.

REFERENCES

- Barstow M. A., et al., 1995, MNRAS, 272, 531
Barstow M. A., O'Donoghue D., Kilkenny D., Burleigh M. R., Fleming T. A., 1995, MNRAS, 273, 711
Bergeron P., Wesemael F., Beauchamp A., Wood M. A., Lamontagne R., Fontaine G., Liebert J., 1994, ApJ, 432, 305
Bloeker T., 1995, A&A, 297, 727
Dobbie P. D., Barstow M. A., Burleigh M. R., Hubeny I., 1999, A&A, 346, 163
Driebe T., Schoenberner D., Bloeker T., Herwig F., 1998, A&A, 339, 123
Finley D. S., Koester D., Basri G., 1997, ApJ, 488, 375
Fontaine G., Wesemael F., 1987, IAU Colloq. 95: Second Conference on Faint Blue Stars, 319-326
Good S. A., Barstow M. A., Holberg J. B., Sing D. K., Burleigh M. R., Dobbie P. D., 2004, MNRAS, 355, 1031
Heber U., Dreizler S., Hagen H.-J., 1996, A&A, 311, L17
Hillwig T. C., Honeycutt R. K., Robertson J. W., 2000, AJ, 120, 1113
Holberg, J.B. and Magargle, 2005, in Proceedings of the NATO Advanced Workshop on White Dwarfs 2004
Holberg J. B., Saffer R. A., Tweedy R. W., Barstow M. A., 1995, ApJ, 452, L133
Koester D., Weidemann V., Schulz H., 1979, A&A, 76, 262
Kruk J. W., Chayer P., Dupuis J., 2003, in Proceedings of the NATO Advanced Workshop on White Dwarfs 2002, de Martino, D., Silvotti, R., Solheim, J.-E. and Kalytis, R. (eds), Kluwer
Moos H. W. et al., 2000, ApJ, 538, L1
Morton D. C., 1991, ApJS, 77, 119
Napiwotzki R., Schöberner D., 1993, In: Barstow M. (ed) 8th European Workshop on White Dwarfs, Kluwer Academic Publishers, p.99
Pounds K. A., et al., 1993, MNRAS, 260, 77
Saffer R. A., Livio M., Yungelson L. R., 1998, ApJ, 502, 394
Sahnou D. J. et al., 2000, ApJ, 538, L7
Sing, D. K., Holberg, J. B., Burleigh, M. R., Good, S. A., Barstow, M. B., Oswald, T. D., Howell, S. B., Brinkworth, C. S., Rudkin, M., Johnston, K., Rafferty, S., 2004, AJ, 127, 2936
Unglaub K., Bues I., 1998, A&A, 338, 75
Unglaub K., Bues I., 2000, A&A, 359, 1042
Vennes S., Pelletier C., Fontaine G., Wesemael F., 1988, ApJ, 331, 876
Vennes S., Thorstensen J. R., 1994, ApJ, 433, L29
Vennes S., Thorstensen J. R., Polomski E. F., 1999, ApJ, 523, 386
Wesemael F., Greenstein J. L., Liebert J., Lamontagne R., Fontaine G., Bergeron P., Glaspey J. W., 1993, PASP, 105, 761